Structural and Energetic Aspects of the Protonation of Phenol, Catechol, Resorcinol, and Hydroquinone

Guy Bouchoux,*[a] Dirk Defaye,[a] Terrance McMahon,[b] Alexander Likholyot,[b] Otilia Mó,[c] and Manuel Yáñez[c]

Abstract: The various protonated forms of phenol (**1**), catechol (**2**), resorcinol (**3**), and hydroquinone (**4**) were explored by ab initio quantum chemical calculations at the MP2/6-31G(d) and B3LYP/6-31G(d) levels. Proton affinities (PA) of **1**–**4** were calculated by the combined G2(MP2,SVP) method, and their gas-phase basicities were estimated after calculation of the change in entropy on protonation. These theoretical data were compared with the corresponding experimental values determined in a high-pressure mass spectrometer. This comparison confirmed that phenols are essentially carbon bases and that protonation generally occurs in a position *para* to the hydroxyl group. Resorcinol is the most effective base (PA = 856 kJ mol^{-1}) due to the participation of both oxygen atoms in the stabilization of the protonated form. Since protonation is accompanied by a freezing of the two internal rotations, a significant decrease in entropy is observed. The basicity of catechol (PA = 823 kJ mol^{-1}) is due to the existence of an intramolecular hydrogen bond, which is strengthened upon protonation. The lower basicity of hydroquinone (PA = 808 kJ mol^{-1}) is a consequence of the fact that protonation necessarily occurs in a position *ortho* to the hydroxyl group. When the previously published data are reconsidered and a corrected protonation entropy is used, a proton affinity value of 820 kJ mol^{-1} is obtained for phenol.

Keywords: ab initio calculations · basicity · mass spectrometry · phenols · protonation

Introduction

Phenols are ubiquitous compounds which present a contrasting array of reactivity that stems from acidic, basic, and redox properties and includes condensation and rearrangement processes.[1] Numerous phenolic compounds are of natural origin and are present in many manufactured products such as, for example, beverages, oils, colorants, and flavorings. Polymerization of natural polyphenols leads to lignin and melanin; moreover, several diphenolic derivatives such as catechins are carcinogen inhibitors. Phenols also form an important class of antioxidants that inhibit the oxidative degradation of organic or bioorganic molecules.[2, 3] Finally, the activity of phenols toward free radicals is of some importance, and their scavenging role is related to their ability to react with radicals much more rapidly than other organic substrates. For example, tocopherol (vitamin E) is an efficient trapping agent which can scavenge damaging peroxy radicals in blood plasma.[4] Given this large range of applications, the determination of the fundamental chemical properties of phenols appears to be of general interest. Therefore, the present study focuses on the intrinsic basicity of isolated phenol and dihydroxybenzenes and on relevant structural aspects.

The gas-phase basicity of phenol (**1**) has been the subject of only a few experimental determinations[5] and, to date, no such measurement has been performed for catechol (**2**), resorcinol (**3**), or hydroquinone (**4**). In the present study, a complete investigation of these four compounds has made by using ab initio molecular orbital calculations up to the G2(MP2,SVP) level. The basicity of dihydroxybenzenes **2**–**4** was determined by measuring their proton transfer equilibrium constants in a high-pressure mass spectrometer (HPMS).

[a] Prof. Dr. G. Bouchoux, D. Defaye
Département de Chimie
Laboratoire des Mécanismes Réactionnels
Ecole Polytechnique
91128 Palaiseau Cedex (France)
Fax: (+33) 1-69-33-30-41
E-mail: bouchoux@dcmr.polytechnique.fr

[b] Prof. Dr. T. McMahon, A. Likholyot
Department of Chemistry
University of Waterloo
Waterloo (Canada)

[c] Prof. Dr. O. Mó, Prof. Dr. M. Yáñez
Departamento de Quimica
Universidad Autonoma de Madrid
Cantoblanco 28049 Madrid (Spain)

  0947-6539/02/0813-2900 $ 17.50+.50/0

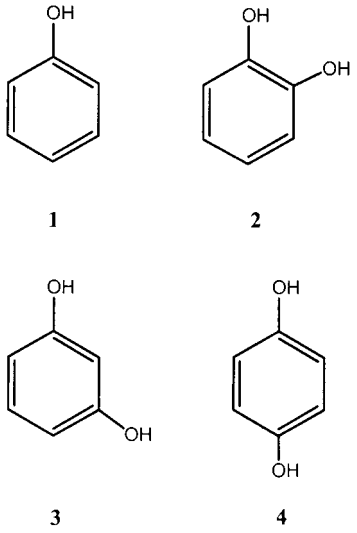

Results and Discussion

Neutral phenol (1): The optimized geometry of neutral phenol is presented in Figure 1. The six C–C bonds are of almost identical length (1.395 ± 0.003 Å, MP2/6-31G(d) and B3LYP/6-31G(d) calculations), and this indicates negligible perturbation of the aromatic ring by the OH group. However, the

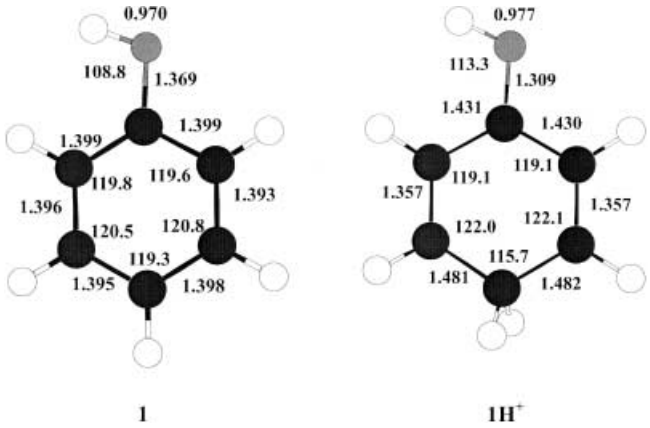

Figure 1. Optimized geometries (B3LYP/6-31G(d) results) of the most stable forms of neutral (**1**) and protonated phenol (**1H**$^+$).

conjugation of one of the electron pairs of the oxygen atom with the π system is evidenced by the shortening of the C–O bond with respect to a pure σ bond (1.375 Å in **1** and 1.425 Å in methanol, for example, MP2/6-31G(d) calculation), and the coplanar arrangement of the OH group and the ring. This latter point is also illustrated by the existence of a non-negligible rotational barrier around the C–O bond. At the MP2/6-31G(d) level, this barrier amounts to 15.0 kJ mol^{-1}, a value which compares nicely with the experimental value of 13.6 kJ mol^{-1}.[14] By comparison, the C–O rotational barrier is only 4.5 kJ mol^{-1} in methanol.[15]

Protonated phenol (1H$^+$): Seven protonated forms of the phenol molecule were identified. The most stable corresponds to protonation at the *para* position of the benzene ring (denoted *p*-**1H**$^+$, Figure 1). In order of decreasing stability, this is followed by the *ortho*-, *O*-, *meta*-, and *ipso*-protonated structures, as summarized in Scheme 1.

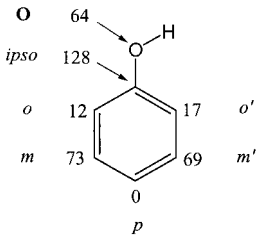

Scheme 1. MP2/6-31G(d) relative energies of the protonated forms of phenol [kJ mol^{-1}].

Structure *p*-**1H**$^+$ is characterized by a shortening of the C–O and C_{ortho}–C_{meta} bonds with respect to the neutral molecule (Figure 1). By contrast, the C_{ortho}–C_{ipso} and C_{meta}–C_{para} bonds are elongated. This was expected for the latter, since a sp^3-hybridized carbon atom is created on protonation in the *para* position. These observations, as a whole, indicate that *p*-**1H**$^+$ can be described essentially by two resonance structures **A** and **B**. A consequence of the extra conjugation of the lone pair of the oxygen atom is the considerable increase in the C–O rotational barrier in *p*-**1H**$^+$ with respect to **1**. At the MP2/6-31G(d) level this barrier amounts to 59.7 kJ mol^{-1}.

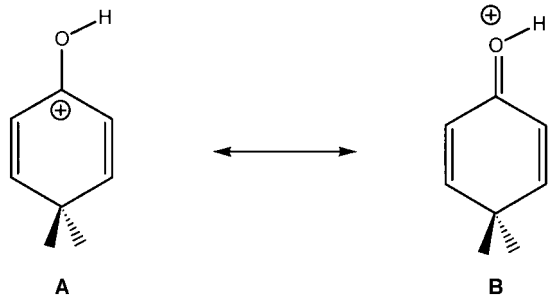

Protonation at the *ortho* positions leads to structures *o*-**1H**$^+$ and *o*′-**1H**$^+$, which lie only 12 and 17 kJ mol^{-1}, respectively, above *p*-**1H**$^+$ (Scheme 1, MP2/6-31G(d) calculations). The slight difference in energy between the two *ortho* conformers *o*-**1H**$^+$ and *o*′-**1H**$^+$ may be explained by the existence of electrostatic interactions between the hydroxyl group and the hydrogen atoms in the *ortho* positions. For example, in structure *o*-**1H**$^+$ a favorable electrostatic interaction arises between the oxygen atom and the two hydrogen atoms of the *ortho*-methylene group (and a repulsive one between the hydrogen atom of the hydroxyl group and the lone *ortho*-hydrogen atom). Similar effects lead to a less pronounced stabilization for *o*′-**1H**$^+$. We note, to support this interpretation, that the C(H$_2$)CO angle is smaller than the C(H)CO angle in *o*-**1H**$^+$ and larger than in *o*′-**1H**$^+$. For both structures a strengthening of the C–O bond and of two C–C bonds is observed, and this points to major participation of the

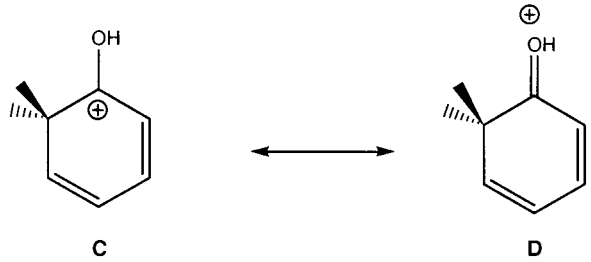

mesomeric forms **C** and **D** in the description of the π-electron delocalization. In line with this description, the barrier for internal rotation around the C–O bond is also higher than 50 kJ mol^{-1}.

Oxygen-protonated phenol (*O*-**1H**$^+$) is less stable than *p*-**1H**$^+$ by 64 kJ mol^{-1}. The prominent structural characteristic of ***O*-1H**$^+$ is the pyramidalization of the oxygen atom; the two hydrogen atoms adopt a position that is symmetric with respect to the plane of the phenyl ring. Consequently, the conjugation of the oxygen atom lone pair with the π system disappears. This is also corroborated by the lengthening of the C–O bond (> 1.50 Å) and by the fact that the C–C bonds have approximately the same length as in the phenol molecule itself.

Protonation at the *meta* position of the phenol molecule leads to structures *m*-**1H**$^+$ and *m*′-**1H**$^+$, situated about 70 kJ mol^{-1} above *p*-**1H**$^+$. The majority of this instability is due to the limited conjugation of the oxygen lone pair with the π system. The C–C bond lengths are very similar in *m*-**1H**$^+$, *m*′-**1H**$^+$, and **1**. Moreover, the C–O bond is only marginally affected by protonation at the *meta* position. It is thus not surprising that the calculated rotational barrier around the C–O bond is 17.2 kJ mol^{-1}, that is, a value close to that of **1**. These observations are in keeping with a description of the π system by the three usual mesomeric forms **E** – **G**.

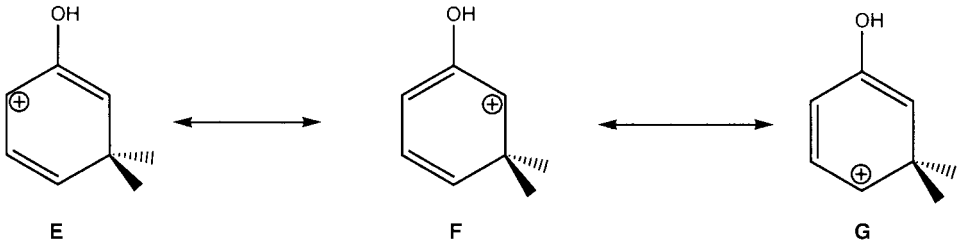

E **F** **G**

Finally, the least favorable protonation site is the *ipso* position, and the structure *i*-**1H**$^+$ is situated 128 kJ mol^{-1} above *p*-**1H**$^+$. In this structure, conjugation of the oxygen lone pair is impossible, and this partly explains its instability. In the calculated structure *i*-**1H**$^+$ the C_{ortho}–C_{meta} bonds are shorter than the C_{meta}–C_{para} bonds, and this indicates a major contribution to the electronic structure by the mesomeric form **H**. We also note the *trans*-coplanar arrangement of the $HOC_{ipso}H$ atoms, which allow a larger distance between the two positively charged hydrogen atoms.

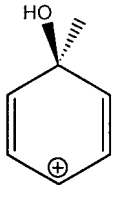

H

Neutral catechol (2): Two conformers of catechol were identified in the calculations. The most stable, **2a** (Figure 2), corresponds to an orientation of the two OH groups that allows formation of an internal hydrogen bond. The second structure **2b** has a repulsive orientation of the two OH dipoles and is destabilized by no less than 19-16 kJ mol^{-1} with respect to **2a**. The intramolecular hydrogen bond in **2a** exhibits a nonnegligible charge density at the bond critical point

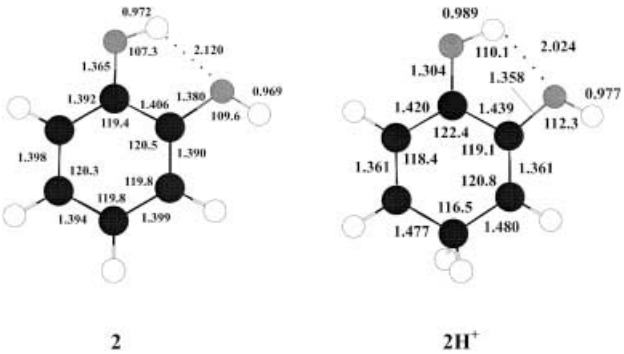

2 **2H**$^+$

Figure 2. Optimized geometries (B3LYP/6-31G(d) results) of the most stable forms of neutral (**2**) and protonated catechol (**2H**$^+$).

(0.018 e au^{-3}), lengthening of the O1–H1 donor bond of 0.004 Å, and a red shift of the corresponding OH stretching frequency of 37 cm^{-1} with respect to phenol, while the stretching frequency of the O2–H2 bond of the acceptor oxygen atom is blue-shifted by 19 cm^{-1}.

As in phenol, the six C–C bonds are approximately of identical length for both **2a** and **2b**. The conjugation of one electron pair of each oxygen atom with the π system is also confirmed here by the shortening of both C–O bonds with respect to pure σ bonds and by the coplanar arrangement of the OH groups and the phenyl ring. The rotational barriers associated with the two hydroxyl groups are, as expected, very different. The rotation of the OH group whose hydrogen atom is involved in the internal hydrogen bond corresponds to the isomerization **2a** → **2b** and is associated with a barrier of 24 kJ mol^{-1} [HF/6-31G(d)]. On the other hand, rotation around the C–O2 bond results in a degenerate rearrangement of **2a**. In fact no considerable change in energy is observed when the CCO2H2 angle is increased; accordingly, the hydrogen atom H1 involved the internal hydrogen bond is simultaneously pushed back and H1 ··· O2 is progressively replaced by an H2 ··· O1 internal hydrogen bond. The transition structure corresponds approximately to a CCOH2 angle of 135° and a CCOH1 angle of 50°. A consequence of this "gearing effect" is that the energy barrier is slightly less than that observed for the phenol itself (10 kJ mol^{-1}, HF/6-31G(d) calculation).

Note that the calculated energy difference between **2a** and **2b** corresponds to a Boltzmann population in which **2b** accounts for only 0.2 % at 298 K. Thus, the measurement of the gas-phase basicity of catechol is essentially related to the conformer **2a**.

Protonated catechol (2H$^+$**)**: The various protonation sites of the most stable conformer of catechol (**2a**) were investigated. For structure **2b**, only the two most probable protonation sites were considered. The relative energies of the corresponding protonated forms are summarized in Scheme 2.

  0947-6539/02/0813-2902 $ 17.50+.50/0 *Chem. Eur. J.* **2002**, *8*, No. 13

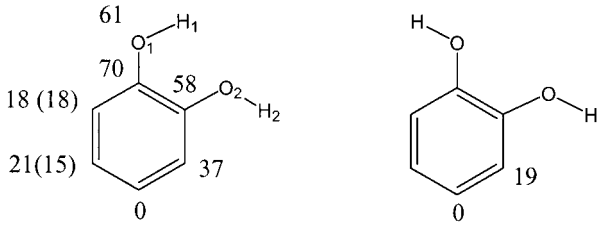

0 25 (20)

Scheme 2. MP2/6-31G(d) and, in parentheses, B3LYP/6-31G(d) relative energies of the protonated forms of catechol [kJ mol^{-1}].

The most stable structure, *p*-**2aH**$^+$ (Figure 2), is protonated in the position *para* to the hydroxyl group O1H1 whose hydrogen atom participates in the hydrogen bond. In fact, this corresponds to the most efficient way to reinforce the internal hydrogen bond (O1H1 $\cdots$ O2). In line with this interpretation, the largest geometrical change occurring from **2a** to *p*-**2aH**$^+$ is the shortening of the H1 $\cdots$ O2 distance. We note also a pronounced shortening of the C–O1 bond, which indicates conjugation of an electron pair of O1 with the phenyl ring. This situation is reminiscent of the protonation of phenol at the *para* position. In contrast the other oxygen atom O2 is not significantly involved in the π-electron delocalization, as was observed for the *meta*-protonated form of phenol. Both effects have the common consequence of strengthening the internal hydrogen bond in *p*-**2aH**$^+$. This latter effect may be described by the resonance structures **I** and **J**.

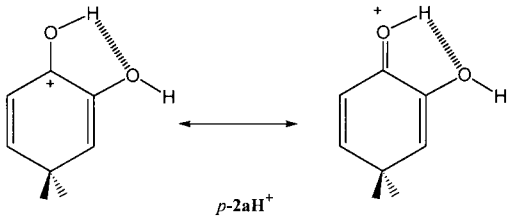

I **J**

The reinforcement of the internal hydrogen bond upon protonation is also reflected in a significant increase in the charge density (0.023 e au^{-3}) at the corresponding bond critical point, by a greater lengthening of the O1H1 donor group (0.014 Å), and by a large red shift (138 cm^{-1}) of its stretching frequency. Accordingly, the in-plane OH bending frequency is also red-shifted by 210 cm^{-1}, while the out-of-plane OH bending frequency is blue-shifted by 292 cm^{-1}. In a similar way, the C–O1 rotational barrier is dramatically increased (73.8 kJ mol^{-1} compared to 24.0 kJ mol^{-1} in the neutral molecule), while a modest change is observed for the C–O2 rotational barrier (17.5 kJ mol^{-1} compared to 10.0 kJ mol^{-1} in neutral catechol).

Protonation at the position *para* to O2H2 leads to *p*′-**2aH**$^+$, which is less stable than *p*-**2aH**$^+$ by 21(15) kJ mol^{-1}. In fact, for structure *p*′-**2aH**$^+$, the π-electron delocalization involves essentially the oxygen atom O2, not O1, as attested to by the shortening of the C–O2 bond and the decrease in electron density on O2. Similarly, the net positive charge on H1 is reduced due to the loss of conjugation of O1 with the phenyl ring.

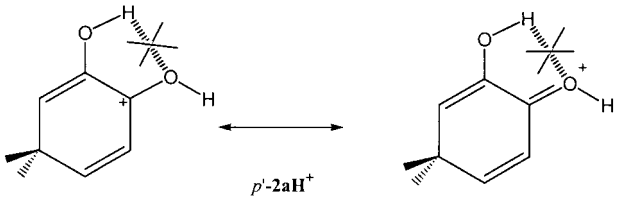

The result is a weakening of the internal hydrogen bond in *p*′-**2aH**$^+$ with respect to *p*-**2aH**$^+$, in agreement with their relative energies. This weakening is so pronounced that no bond critical point can be found between H1 and O2, and the red shift of the OH donor stretching frequency with respect to the neutral molecule is practically zero, while the out-of-plane OH bending is red-shifted (by 63 cm^{-1}) rather than blue-shifted.

Comparable arguments can be used to explain the energy difference of 19 kJ mol^{-1} between the two *ortho*(*meta*) protonated forms of catechol *o*-**2aH**$^+$ and *o*′-**2aH**$^+$:

Note, however, that the *o*-**2aH**$^+$ and *p*′-**2aH**$^+$ forms are of comparable energy because the former again has an intramolecular hydrogen bond that is stronger than that of the neutral molecule, and therefore much stronger than that of the latter. The charge density at the bond critical point in *o*-**2aH**$^+$ is 0.020 e au^{-3}, the lengthening of the O1H1 donor is 0.013 Å, the O1H1 stretching band is red-shifted by 125 cm^{-1}, and the out-of-plane O1H1 bend is blue-shifted by 258 cm^{-1}.

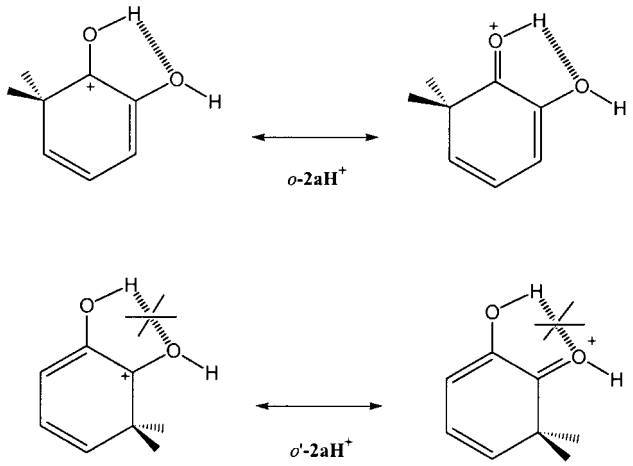

The *ipso*-protonated forms of **2a** lie only 58 and 70 kJ mol^{-1} above *o*-**2aH**$^+$. These relative energies are very different from the energy difference of 128 kJ mol^{-1} calculated between the two analogous protonated forms of phenol *i*-**1H**$^+$ and *p*-**1H**$^+$. The spectacular stabilization of the most stable *ipso*-protonated form of **2a**, *i*-**2aH**$^+$, is clearly related to the presence of the second hydroxyl group. Accordingly, the oxygen atom O2 is completely involved in the π delocalization, and an internal hydrogen bond is still present in this structure.

As for phenol, the *O*-protonation of catechol leads to pyramidalization of the corresponding oxygen atom, and the two hydrogen atoms adopt a position symmetrical with respect to the plane of the phenyl ring that allows two favorable electrostatic interactions with the second oxygen atom.

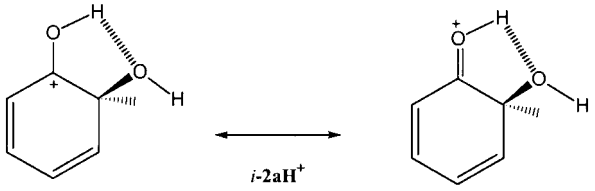

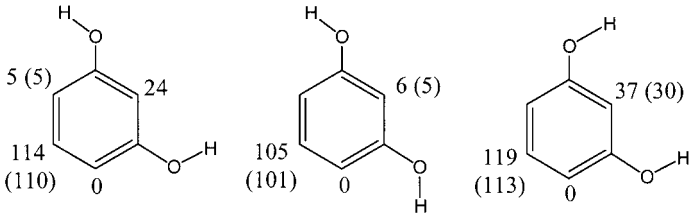

3a 0 **3b** 8 (6) **3c** 1 (2)

Scheme 3. MP2/6–31G(d) and, in parentheses, B3LYP/6-31G(d) relative energies of the protonated forms of resorcinol [kJ mol^{-1}]

Finally, protonation in the *para* position of conformer **2b** leads to structure *p*-**2bH**$^+$, which lies 25(20) kJ mol^{-1} above *p*-**2aH**$^+$,in line with the lack of an internal hydrogen bond.

Neutral resorcinol (3): The three conformers of resorcinol (Scheme 3) **3a**–**3c** have very similar energies, and this is indicative of negligible interactions between the two hydroxyl groups. Each of these three forms is separated from its neighbor by a rotational barrier of about 15 kJ mol^{-1}, as in the case of phenol.

Protonated resorcinol (3H$^+$): The most favored protonation site of resorcinol is on a carbon atom *para* to one of the hydroxyl groups (and hence *ortho* to the other; Figure 3). The relative energies of the *ortho*-, *meta*-, and *para*-protonated forms of the three conformations of neutral resorcinol are displayed in Scheme 3. The most stable structures **3aH**$^+$, **3bH**$^+$, and **3cH**$^+$ have very similar energies, as indicated in Scheme 3. Oxygen- and *ipso*-protonated forms lie about 110 and 170 kJ mol^{-1}, respectively, above **3aH**$^+$, **3bH**$^+$, and **3cH**$^+$.

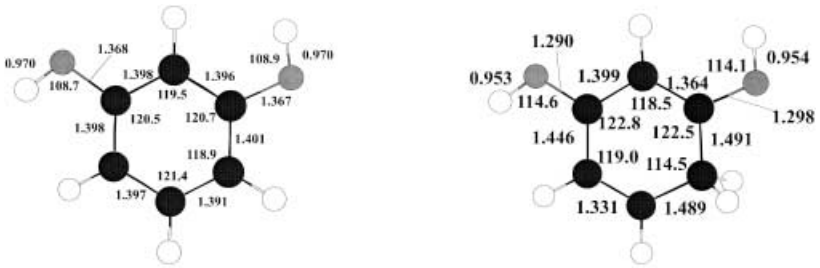

3 **3H**$^+$

Figure 3. Optimized geometries (B3LYP/6-31G(d) results) of the most stable forms of neutral (**3**) and protonated resorcinol (**3H**$^+$).

Two *para*-protonated structures were found for neutral **3a**, *p*-**3aH**$^+$ and *p*′-**3aH**$^+$, while, for symmetry reasons, only *p*-**3bH**$^+$ and *p*-**3cH**$^+$ can be formed from neutral **3b** and **3c** (Figure 3). The four protonated forms have very similar energies (in a 6 kJ mol^{-1} range at the B3LYP level) and are characterized by the participation of both oxygen atoms in the π-electron delocalization. This is attested to by the shortening of the C–O bonds and by the similar high rotational barriers (HF/6-31G(d) calculations lead to values of 45.8 kJ mol^{-1} and 49.5 kJ mol^{-1} for the two rotational barriers of structure *p*-**3aH**$^+$). The description of the π-electron clouds of the *para*-protonated forms of resorcinol requires more than two limiting forms (**K**–**N**).

The slight differences in stability between the four *para*-protonated conformers of resorcinol are easily understood from electrostatic arguments. For example, it is reasonable to assume that *p*-**3aH**$^+$ is slightly more stable than *p*′-**3aH**, because in the former the two hydrogen atoms attached to the protonated center have a stabilizing interaction with the OH group that is closer to them, while in the latter there is a repulsive interaction between these two hydrogen atoms and that on the nearby hydroxyl group.

The second type of protonated structure easily formed from resorcinol is obtained by protonation at the position *ortho* to both hydroxyl groups. Clearly, structure *o*-**3bH**$^+$ is energetically favored because the two hydrogen atoms of the hydroxyl groups are distant from the methylene group created by the incoming proton. The electrostatic repulsion of the positive charges borne by the hydrogen atoms is thus minimized. The situation is not so favorable for *o*-**3aH**$^+$ and, more dramatically, for *o*-**3cH**$^+$. Despite these differences, the *ortho*-protonated forms of resorcinol are stabilized by the participation of the two oxygen atoms in the π-electron delocalization (**O**–**R**). This stabilizing effect is not efficient in the *meta*- or *ipso*-protonated forms of resorcinol, as is illustrated by their high (>110 kJ mol^{-1}) energies relative to *p*-**3aH**$^+$.

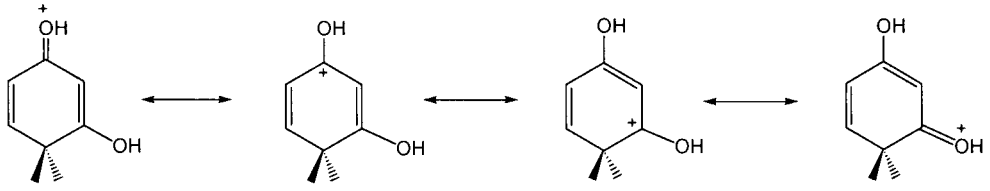

K **L** **M** **N**

0947-6539/02/0813-2904 $ 17.50+.50/0 *Chem. Eur. J.* **2002**, *8*, No. 13

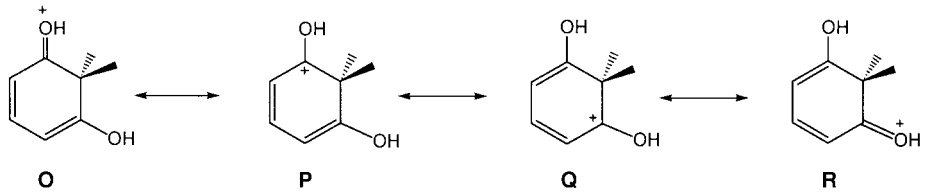

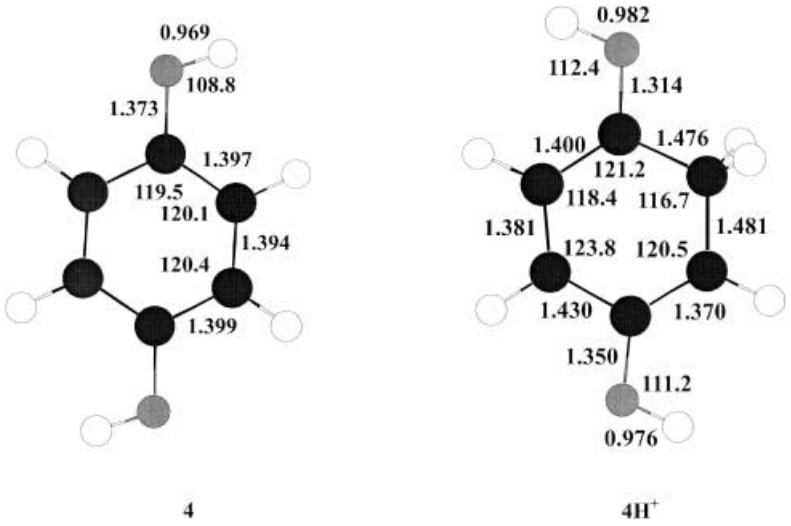

Figure 4. Optimized geometries (B3LYP/6-31G(d) results) of the most stable forms of neutral (**4**) and protonated hydroquinone (**4H**$^+$).

Neutral hydroquinone (4): The two conformers of neutral hydroquinone **4** (Scheme 4), **4a** and **4b**, have quasi-identical energies. The rotational barrier of 6.2 kJ mol^{-1} separating these two species is lower than that calculated at the same level of theory for phenol [11.1 kJ mol^{-1}, HF/6-31G(d)]. This may be interpreted by a decrease in the participation of the oxygen lone pairs in the π-electron delocalization. In fact, the second oxygen atom limits the π-donating effect of the former, as expected from a simple consideration of the Lewis limiting forms.

Protonated hydroquinone (4H$^+$): The most favorable protonation sites of hydroquinone are the four unsubstituted carbon atoms, which are each in a position *ortho* to one of the hydroxyl groups. Slight differences in stability are observed depending on the orientation of the hydroxylic hydrogen atoms (Scheme 4).

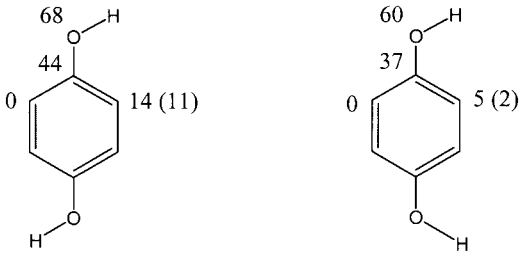

4a **4b**

Scheme 4. MP2/6–31G(d) and, in parentheses, B3LYP/6-31G(d) relative energies of the protonated forms of hydroquinone [kJ mol^{-1}].

Protonation at the *ortho* carbon atom opposite to the hydroxylic hydrogen atom leads to the most stable protonated form (Figure 4), a situation reminiscent of that encountered for phenol itself (Scheme 1). After protonation, the oxygen atom closer to the protonation site becomes involved in the π-electron delocalization. This is in agreement with a representation of the corresponding protonated structure.

The rotational barriers also reflect the different behavior of the two oxygen atoms. For structure *o*-**4H**$^+$, we find 51.7 kJ mol^{-1} for C–O1 and 20.1 kJ mol^{-1} for C–O2 (HF/6-31G(d) calculations).

Protonation at the *ipso* position is significantly easier for hydroquinone than for its two isomers **2** and **3**. This is due to the stabilizing effect of the second hydroxyl group on the positive charge, as illustrated by the resonant forms below.

A similar effect was observed for the *ipso* protonation of catechol (see above).

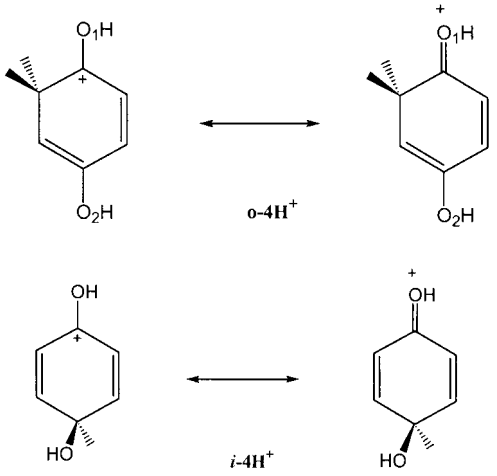

Protonation energetics: Gas-phase basicity GB(M) and proton affinity PA(M) of a molecule M (i.e., the Gibbs free energy and the enthalpy changes, respectively, of the reaction $MH^+ \rightarrow M + H^+$) are interrelated by Equation (1), where $\Delta_p S^\circ$

$$PA(M) = GB(M) + T[\Delta_p S^\circ - S^\circ(H^+)] \quad (1)$$

is the entropy difference $S^\circ(MH^+) - S^\circ(M)$. The influence of this latter term is significant when important structural

changes occur during the protonation process. However, a complete calculation of the third law entropies $S^\circ(MH^+)$ and $S^\circ(M)$ supposes the knowledge of the geometries and relative energies of the various conformers of both M and MH^+ and of their vibrational frequencies and rotational barriers with sufficient accuracy.[16] For the four systems considered, this is a complicated task in view of the size of the molecules and the number of conformers. Here we adopt a semiquantitative treatment which makes allowance for the most meaningful features of the protonation process. The Δ_pS° can be separated into the three usual translational, rotational, and vibrational components. For the systems studied here, we verified that the sum of the translational and rotational terms is negligible (except when M and MH^+ have different symmetry numbers). Thus, only the vibrational contribution to Δ_pS° must be considered. For phenol (**1**) and dihydroxybenzenes **2**–**4**, the preceding section showed that the main modification observed upon protonation is an increase in the rotational barriers associated with the hydroxyl group. Thus, a major component of the entropy difference $\Delta_pS^\circ = S^\circ(MH^+) - S^\circ(M)$ should correspond to these torsional modes. To estimate these contributions, we used the hindered rotor model developed by Pitzer and Gwinn.[17] In this approach, the energy levels of a rotor associated with a potential energy barrier of the form $V_0/2(1-\cos n\phi)$, where ϕ is the dihedral angle, are found with the help of a one-dimensional Schrödinger equation. In practice the calculated entropy of a given rotor S°_{Pitzer} is close to that calculated by using the harmonic oscillator approximation S°_{ho} when V_0 exceeds about 50 kJ mol^{-1} (i.e., $20\,RT$ at 298 K). For lower V_0 values, S°_{Pitzer} is greater than S°_{ho} and tends toward the value corresponding to the free rotation model when $V_0 = 0$. The second contribution to the vibrational part of Δ_pS° originates from the fact that MH^+ has three more vibrational modes. Since the most stable forms considered here correspond to *C*-protonation, the three expected modes should correspond to a C–H bond elongation and two CH_2 deformations. Considering the standard wavenumbers of 3000, 1450, and 850 cm^{-1}, the contribution to Δ_pS° is about 1 J mol^{-1} K^{-1}. A summary of the Δ_pS° calculated by using these approximations is given in Table 1. A possible estimate of the error introduced on Δ_pS° by the above approximation is about 5 J mol^{-1} K^{-1}. For the four compounds considered here, the term Δ_pS° is always negative because *C*-protonation hinders rotation of the hydroxyl group (see above). In hydroquinone (**4**), however, this decrease in entropy on passing from the neutral to the protonated form is partly counterbalanced by the lowering of S°(**4**) due to its symmetry number of two.

Table 1. Summary of the calculation of the entropy difference Δ_pS° [J mol^{-1} K^{-1}] for **1**–**4**[a].

	M		MH^+		Δ_pS°
	V_0[b]	S°_{Pitzer}[c]	V_0[b]	S°_{Pitzer}[c]	Δ_pS°[d]
phenol	13.6	6.8	55.7	1.5	−4.3
catechol	24.0	9.3	73.8	2.6	
	10.0	8.4	17.5	7.0	−7.1 [−4.5]
resorcinol	14.6	11.7	45.8	6.7	
	14.6	11.7	49.5	6.4	−9.3 [−8.9]
hydroquinone	6.2	15.4	51.7	6.2	
	6.2	15.4	20.1	10.1	−7.7 [−5.3]

Very few experimental determinations of the basicity of phenol in the gas phase have been reported in the literature.[5] The gas-phase basicity (GB) and the proton affinity (AP) of phenol reported in the recent compilation by Hunter and Lias[5c] are GB(phenol) = 786.3 kJ mol^{-1} and PA(phenol) = 817.3 kJ mol^{-1}. The GB was derived from two experimental determinations of proton transfer equilibrium constants at a single temperature (537[5b] and 650 K[5a–c]) and corrected to 298 K by using Equation (2), where Δ_TG° is the Gibbs free energy of the reaction $MH^+ + B \rightarrow M + BH^+$ at temperature T, $\Delta_pS^\circ(M) = S^\circ(MH^+) - S^\circ(M)$ and $\Delta_pS^\circ(B) = S^\circ(BH^+) - S^\circ(B)$. The proton affinity is then calculated from Equation (3), where $S^\circ(H^+) = 108.8$ J K^{-1} mol^{-1} at 298 K.

$$GB(M) = GB(B) + \Delta_TG^\circ - (T-298)[\Delta_pS^\circ(M) - \Delta_pS^\circ(B)] \quad (2)$$

$$PA(M) = GB(M) + 298[S^\circ(M) + S^\circ(H^+) - S^\circ(MH^+)] = GB(M) + 298[S^\circ(H^+) - \Delta_pS^\circ(M)] \quad (3)$$

Acording to the original data of Mautner,[5b] proton transfer equilibria between phenol and acetone or naphthalene are associated with $\Delta_{537}G^\circ$ of +2.5 kJ mol^{-1} and −0.4 kJ mol^{-1}, respectively. Using Δ_pS°(phenol) = −4.3 J K^{-1} mol^{-1} (see above), Δ_pS°(acetone) = 8.7 J K^{-1} mol^{-1}[5c] and Δ_pS°(naphthalene) = 30 J K^{-1} mol^{-1}[5c] and the gas-phase basicities GB(acetone) = 782.1 kJ mol^{-1} and GB(naphthalene) = 779.4 kJ mol^{-1} we obtain GB(phenol) = 787.5 ± 0.4 kJ mol^{-1} Similarly, using $\Delta_{650}G^\circ = -32.2$ kJ mol^{-1} for proton transfer between protonated phenol and ammonia[5c] a value of 786.1 kJ mol^{-1} can be deduced for GB(phenol). In summary, the available experimental data combined with our estimate of Δ_pS°(phenol)[18] lead to the following averaged values: GB(phenol) = 786.8 ± 0.7 kJ mol^{-1} and consequently PA(phenol) = 820.5 ± 0.7 kJ mol^{-1}.

For the three dihydroxybenzenes **2**–**4**, equilibrium constants for reactions (b)–(d) measured at different temperatures are shown in the form of van't Hoff plots in Figure 5.

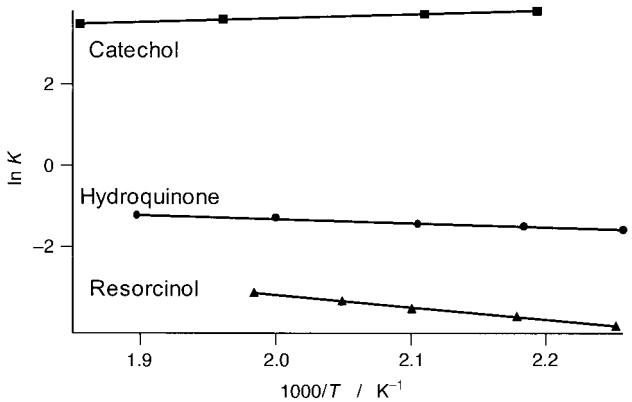

Figure 5. Van't Hoff plot for proton exchange between catechol, resorcinol, and hydroquinone with dimethyl sulfide and nitrobenzene [reactions (b)–(d)].

The enthalpy and entropy changes for reactions (b)–(d) calculated from the van't Hoff plots are given in Table 2 together with absolute proton affinities and entropy differences Δ_pS° for **2**–**4**.

0947-6539/02/0813-2906 $ 17.50+.50/0 *Chem. Eur. J.* **2002**, *8*, No. 13

Table 2. Experimental enthalpy and entropy changes ΔH° and ΔS° for reactions $MH^+ + B \rightarrow M + BH^+$ and related proton affinity (PA) and entropy difference $\Delta_p S^\circ$.[a]

M	B	ΔH°	ΔS°	PA	$\Delta_p S^\circ$
catechol	dimethyl sulfide	-8.0 ± 1.2	14 ± 3	822.9	-5
resorcinol	dimethyl sulfide	25.4 ± 1.6	24 ± 3	856.4	-15
hydroquinone	nitrobenzene	8.1 ± 1.6	5 ± 4	808.4	0

[a] Units for enthalpies and entropies are $kJ\,mol^{-1}$ and $J\,mol^{-1}K^{-1}$, respectively. [b] PA and $\Delta_p S^\circ$ calculated from data for reference compounds from ref. [5c].

Considering the temperature range used for the van't Hoff experiments, the ΔS° and $\Delta_p S^\circ$ terms correspond to a mean temperature of about 490 K. Hence, a theoretical estimate of the latter was made at this temperature (see Table 2, values in brackets). The comparison of the $\Delta_p S^\circ$ obtained theoretically (Table 1) and experimentally (Table 2) is excellent given the uncertainties in both sets of data (i.e., ca. 5 $J\,mol^{-1}K^{-1}$).

To estimate the proton affinity of **1**–**4** as accurately as possible, we used the G2(MP2,SVP) method and the cheaper B3LYP/6-311 + G(3df,2p) procedure. The results are summarized in Tables 3 and 4. A direct estimate of the proton affinity is simply given by Equation (6). The results (Table 4, columns a) indicate that for the phenol (**1**) and the dihydroxybenzenes **2**–**4**, G2(MP2,SVP) underestimates the proton affinity by 6 ± 2 $kJ\,mol^{-1}$, while the B3LYP/6-311 + G(3df,2p) approach overestimates this quantity by 11 ± 4 $kJ\,mol^{-1}$. A similar observation was made for the benzene molecule, for which the deviations between theory and experiment are -7.6 and $+14.7$ $kJ\,mol^{-1}$ for G2(MP2,SVP) and B3LYP/6-311 + G(3df,2p) methods, respectively. It was consequently of interest to find a more precise theoretical estimate of the proton affinities of **1**–**4**. Recently, it was claimed that B3LYP yields reliable proton affinities when used with a 6-311 + G(3df,3pd) basis set.[11] However, for catechol we found that the protonation energy evaluated at this level differs from the B3LYP/6-311 + G(3df,2p) value by less than 1 $kJ\,mol^{-1}$. Hence, the larger basis set is not expected to significantly improve the theoretical estimate of the proton affinities of the molecules considered here.

Another approach is to consider isodesmic reactions such as the proton transfer process between the protonated molecule of interest and a reference base B ($MH^+ + B \rightarrow M + BH^+$). The proton affinity deduced from this isodesmic reaction is simply given by $PA_{iso}(M) = PA_{calcd}(M) + PA_{exp}(B) - PA_{calcd}(B)$. Using the benzene molecule as the reference base B, (PA_{exp}(benzene) = 750.4 $kJ\,mol^{-1}$[5c]) we obtained the results quoted in columns b in Table 4. The agreement between theory and experiment is clearly improved. On average, isodesmic PAs calculated at the G2(MP2,SVP) or the B3LYP/6-311 + G(3df,2p) level with reference to benzene differ from experiment by less than 4 $kJ\,mol^{-1}$. Note that G2(MP2,SVP) leads to proton affinity values which are slightly higher than those given by the B3LYP/6-311 + G(3df,2p) method. When phenol is used as reference base B in the isodesmic calculation, the deviation between theory and experiment is not improved, but is still very good, since the average deviation (5.5 $kJ\,mol^{-1}$) is within the limits of "chemical accuracy".

Conclusion

Good agreement between theory and experiment was found for GB, PA, and $\Delta_p S^\circ$, that is, the structural assignment of both

Table 3. Summary of the energy calculations of benzene, phenol, catechol, resorcinol, and hydroquinone (in Hartree).

	Benzene	BenzeneH^+	Phenol	PhenolH^+	Catechol	CatecholH^+	Resorcinol	ResorcinolH^+	Hydroquinone	HydroquinoneH^+
HF/6-31G(d)	−230.70314	−231.01468	−305.55806	−305.89698	−380.41296	−380.75182	−380.41477	−381.76870	−380.40950	−380.74173
ZPE · 0.893[a]	0.09615	0.10604	0.10029	0.11170	0.10437	0.11586	0.10454	0.11659	0.10410	0.11464
$H^\circ_{298} - H^\circ_0$[b]	0.00504	0.00568	0.00613	0.00641	0.00738	0.00759	0.00719	0.00730	0.00745	0.00723
MP2/6-31G(d)	−231.45773	−231.75031	−306.49099	−306.80983	−381.52587	−381.84800	−381.52452	−381.8600	−381.52191	−381.83714
QCISD(T)/6-31G(d)	−231.53139	−231.83256	−306.56881	−306.89721	−381.60726	−381.93900	−381.60670	−381.95108	−381.60346	−381.92822
MP2/6-311 + G(3df,2p)	−231.72047	−232.00299	−306.84651	−307.15505	−381.97400	−382.28528	−381.97145	−382.29654	−381.97006	−382.27440
G2(MP2,SVP)[c]	−231.7778	−232.05899	−306.91979	−307.22649	−382.06274	−382.38214	−382.06081	−382.38275	−382.05923	−382.36256
B3LYP/6-311 + G(3df,2p)	−232.32751	−232.62712	−307.58063	−307.90481	−382.83394	−383.16103	−382.83309	−383.17316	−382.83059	−383.15198

[a] Zero-point vibrational energy scaled by a factor of 0.893. [b] HF/6-31G(d) thermal correction to enthalpy at 298 K (unscaled). [c] Including the higher level correction (HLC) terms of −0.0798, −0.09576, and −0.11172 Hartree for benzene, phenol, and diphenols, respectively.

Table 4. Calculated and experimental proton affinity [$kJ\,mol^{-1}$] at 298 K of benzene, phenol, catechol, resorcinol, and hydroquinone.

Level	Benzene	Phenol		Catechol			Resorcinol			Hydroquinone		
	a	a	b	a	b	c	a	b	c	a	b	c
HF/6-31G(d)	796.5	865.2	819.1	865.1	819.0	820.4	903.5	857.4	858.8	851.3	805.2	806.6
MP2/6-31G(d)	746.7	812.5	816.2	821.2	824.9	829.2	855.0	858.7	863.0	806.7	810.4	814.7
QCISD(T)/6-31G(d)	769.2	837.6	818.8	846.4	827.6	829.3	878.4	859.6	861.3	831.7	812.9	814.6
MP2/6-311 + G(3df,2p)	720.3	785.5	815.6	792.7	822.8	827.7	827.7	857.8	862.7	778.1	808.2	813.1
G2(MP2,SVP)	742.8	810.6	818.2	817.9	825.5	827.8	851.1	858.7	861.0	803.1	810.7	813.0
B3LYP/6-311 + G(3df,2p)	765.1	826.6	811.9	834.2	819.5	828.1	867.1	852.4	861.0	822.9	808.2	816.8
Experimental	750.4	820.5			822.9			856.4			808.4	

[a] Direct calculation with Equation (6) at the level of theory indicated in the first column by using the HF/6-31G(d) zero-point vibrational energy scaled by a factor of 0.893 and the HF/6-31G(d) thermal correction at 298 K (unscaled). [b] Isodesmic estimate based on PA(benzene) = 750.4 $kJ\,mol^{-1}$. [c] Isodesmic estimate based on PA(phenol) = 820.5 $kJ\,mol^{-1}$.

the neutral and protonated structures by molecular orbital calculations is essentially correct. In particular, the results confirm unambiguously that phenols are carbon bases and that regiospecific protonation generally occurs *para* to the hydroxyl group.

Protonation of phenol in the *para* position is favored over the *ortho* position by about 15 kJ mol^{-1}. Resorcinol is the more effective base due to the participation of both oxygen atoms in stabilizing the protonated form by donating electrons to the π-electron system. Protonation is accompanied by a freezing of the two internal rotations and thus leads to a significant decrease in entropy.

As bases, catechol and hydroquinone are slightly more and slightly less effective than phenol, respectively. The stronger basicity of the former is due to the existence of an internal hydrogen bond, which is strengthened after protonation. The lower basicity of hydroquinone is due to the fact that protonation occurs necessarily in a position *ortho* to one hydroxy group.

Experimental Section and Methods of Calculation

Experimental: The experimental studies of proton exchange equilibria involving dihydroxybenzenes **2**–**4** [A in Eq. (a)] and reference bases B were performed with a pulsed electron beam, variable-temperature, high-

$$AH^+ + B \rightarrow A + BH^+ \quad (a)$$

pressure mass spectrometer at the University of Waterloo.[6] The equilibrium constant for reaction (a) is given by Equation (4)), where I_x are ionic abundances and [A] and [B] represent the relative proportions of A and B.

$$K = I_{BH^+}[A]/I_{AH^+}[B] \quad (4)$$

Several compounds were tested as proton exchange partners in these reactions. The selection criteria were based on the requirement that an exchange partner does not participate in competing reactions, such as proton-bound dimer formation, to any significant extent and that its proton affinity is close to the calculated proton affinity of the studied dihydroxybenzene, generally within 10 kJ mol^{-1}. The latter requirement was to ensure that ratios of neutral compound concentrations and measured ionic ratios are within the range 1–10. The exchange partners finally chosen were dimethyl sulfide for catechol and resorcinol and nitrobenzene for hydroquinone [Eqs. (b)–(d)].

$$1,2\text{-}C_6H_6O_2H^+ + (CH_3)_2S \rightarrow 1,2\text{-}C_6H_6O_2 + (CH_3)_2SH^+ \quad (b)$$

$$1,3\text{-}C_6H_6O_2H^+ + (CH_3)_2S \rightarrow 1,3\text{-}C_6H_6O_2 + (CH_3)_2SH^+ \quad (c)$$

$$1,4\text{-}C_6H_6O_2H^+ + C_6H_5NO_2 \rightarrow 1,4\text{-}C_6H_6O_2 + C_6H_5NO_2H^+ \quad (d)$$

All three isomers of dihydroxybenzene are crystalline at room temperature and have melting points of 104 °C for catechol, 110 °C for resorcinol, and 170 °C for hydroquinone. The sample mixtures were prepared as follows. A small weighed amount (ca. 70 mg) of a dihydroxybenzene was placed in a 5-L stainless steel vessel of the gas-handling plant at room temperature. The vessel was then evacuated and filled with methane, which was used as a carrier/buffer gas. Selected exchange partners were injected into the 5-L vessel with a calibrated syringe through a fitted septum port. The gas-handling plant was subsequently heated to 5–10 °C above the melting temperature of the dihydroxybenzene and left for 10 h to ensure complete vaporization of the dihydroxybenzene. The sample mixture was then allowed to flow through the ion source. To prevent deposition of dihydroxybenzenes on the walls of the gas transfer lines connecting the gas handling plant and the ion source, the lines were heated to above 100 °C. This measure proved to be crucial for dihydroxybenzenes to reach the ion source. Nevertheless, two cold spots, albeit with a small surface area, could not be eliminated, and a later inspection showed that a small amount of dihydroxybenzenes condensed there. However, the resulting error in the concentration of the neutral compound leads to a systematic error only in the entropy change for a proton exchange reaction that was estimated to be no more than about 4 J mol^{-1} K^{-1}. The proton exchange equilibria were measured over the temperature range 170–270 °C.

Calculations: Standard ab initio molecular orbital calculations were carried out with the Gaussian 98 suite of programs.[7] Both correlated methods and density functional theory (DFT) were used. In the former approach, the geometries of the different species were first optimized at the HF/6-31G* level; the zero-point energy (ZPE) was calculated at this level after scaling by a factor of 0.8929. The geometries were then refined at the MP2(FrozenCore)/6-31G* level to take electron correlation effects explicitly into account. It was established that accurate heats of formation (i.e., ±6 kJ mol^{-1}) can be obtained from calculations at the G2 level of theory or its variant, G2(MP2) and G2(MP2,SVP).[8] Owing to the size of the systems considered, we chose the G2(MP2,SVP) technique. In this approach, the energies are calculated at the QCISD(T) level by using the split-valence plus polarization (SVP) 6-31G(d) basis set. Corrections for basis set deficiencies are evaluated at the MP2/6-311 + G(3df,2p) level. A higher-level correction (HLC), which depends on the number of paired and unpaired electrons, is finally introduced. The total energy E[G2(MP2,SVP)] is then given by Equation (5). The HLC correction is calculated from $HLC = -An_\beta - Bn_\alpha$, where n_β and n_α are the number of β and α valence electrons, respectively ($n_\beta < n_\alpha$), and the parameters A and B are equal to 5.13×10^{-3} and 0.19×10^{-3} Hartree, respectively.

$$E[G2(MP2,SVP)] = E[QCISD(T)/6\text{-}31G(d)] + E[MP2/6\text{-}311 + G(3df,2p)] - E[MP2/6\text{-}31G(d)] + HLC + ZPE \quad (5)$$

It is known that density functional theory may provide accurate results at lower cost. It is well established, for instance, that the B3LYP method yields vibrational frequencies in better agreement with experiment than the MP2 values, at a much lower computational cost.[9] The same good performance is observed for infrared intensities.[10] On the other hand, this DFT approach, when used with a 6-311 + G(3df,2p) basis set expansion, provides PAs in reasonable agreement with the experimental values.[11] Here a comparison is made between G2(MP2,SVP) results and single point energy calculations at the B3LYP/6-311 + G(3df,2p) level with B3LYP/6-31G(d) optimized geometries. The zero-point energy correction was included by using the B3LYP/6-31G(d) vibrational frequencies scaled by a factor 0.98.[12]

The 298 K proton affinities were calculated from Equation (6), where E represents the total energy at 0 K, $\Delta_{298}H^\circ$ the difference $(H^\circ_{298}(M) - H^\circ_0(M)) - [H^\circ_{298}{}^\circ{}_{298}(MH^+) - H^\circ_0(MH^+)]$, and 6.2 kJ mol^{-1} is the enthalpy of translation of the proton at 298 K (i.e., 5/2 RT). The $\Delta_{298}H^\circ$ terms were estimated by using the standard statistical thermodynamic equations and the relevant vibrational frequencies.

$$PA(M) = E(M) - E(MH^+) + \Delta_{298}H^\circ + 6.2 \text{ kJ mol}^{-1} \quad (6)$$

The bonding characteristics of the compounds under investigation, in particular the existence and strength of intramolecular hydrogen bonds in the case of catechol, were analyzed with the atoms in molecules (AIM) theory of Bader.[13] For this purpose the relevant bond critical points (i.e., points where the electron density is minimum along the bond path and maximum in the other two directions) were located, and the values of the electron density at this point were evaluated. A positive value of the latter means a bonding effect, typically, electron density lower than 0.1 e au^{-3} corresponds to weak interactions such as hydrogen bonds, while larger values are associated with covalent bonds.

[1] Z. Rappoport, "The Chemistry of Phenols" in *The Chemistry of Functional Groups*, Wiley, New York, **2002**, in press.

[2] B. Halliwell, J. M. C. Gutteridge, *Free Radical in Biology and Medicine*, 2nd ed., Clarendon Press, Oxford, **1989**.

[3] G. Scott, *Atmospheric Oxidation and Antioxidants*, Elsevier, Amsterdam, **1993**.

[4] G. W. Burton, K. U. Ingold, *Acc. Chem. Res.* **1986**, *19*, 194.

[5] a) Y. K. Lau, P. Kebarle, *J. Am. Chem. Soc.* **1976**, *98*, 7452; b) M. Mautner, *J. Phys. Chem.* **1980**, *84*, 2716; c) E. P. Hunter, S. G. Lias, *J. Phys. Chem. Ref. Data*, **1998**, *27*, 413.

[6] J. E. Szulejko, T. B. McMahon, *Int. J. Mass Spectrom. and Ion Proc.*, **1991**, *109*, 279.

0947-6539/02/0813-2908 $ 17.50+.50/0 *Chem. Eur. J.* **2002**, *8*, No. 13

[7] Gaussian 98, Revision A.6, M. J. Frisch, G. W. Trucks, H. B. Schlegel, G. E. Scuseria, M. A. Robb, J. R. Cheeseman, V. G. Zakrzewski, J. A. Montgomery, Jr., R. E. Stratmann, J. C. Burant, S. Dapprich, J. M. Millam, A. D. Daniels, K. N. Kudin, M. C. Strain, O. Farkas, J. Tomasi, V. Barone, M. Cossi, R. Cammi, B. Mennucci, C. Pomelli, C. Adamo, S. Clifford, J. Ochterski, G. A. Petersson, P. Y. Ayala, Q. Cui, K. Morokuma, D. K. Malick, A. D. Rabuck, K. Raghavachari, J. B. Foresman, J. Cioslowski, J. V. Ortiz, B. B. Stefanov, G. Liu, A. Liashenko, P. Piskorz, I. Komaromi, R. Gomperts, R. L. Martin, D. J. Fox, T. Keith, M. A. Al-Laham, C. Y. Peng, A. Nanayakkara, C. Gonzalez, M. Challacombe, P. M. W. Gill, B. Johnson, W. Chen, M. W. Wong, J. L. Andres, C. Gonzalez, M. Head-Gordon, E. S. Replogle, J. A. Pople, Gaussian, Inc., Pittsburgh PA, **1998**.
[8] L. A. Curtiss, K. Raghavachari, P. C. Redfern, J. A. Pople, *J. Chem. Phys.* **1997**, *106*, 1063.
[9] M. W. Wong, *Chem. Phys. Lett.* **1996**, *256*, 391.
[10] P. J. Stephens, F. J. Devlin, C. F. Chabalowski, M. J. Frisch, *J. Phys. Chem.* **1994**, *98*, 11623.
[11] B. Amekraz, J. Tortajada, J-P. Morizur, A. I. Gonzalez, O. Mo, M.Yanez, I. Leito, P-C. Maria, J.-F. Gal, *New J. Chem.*, **1996**, *20*, 1011.
[12] A. P. Scott, L. Radom, *J. Phys. Chem.*, **1996**, *100*, 16502.
[13] R. F. W. Bader, *Atoms in Molecules. A Quantum Theory*, Clarendon Press, Oxford, **1990**.
[14] *Internal Rotation in Molecules*, (Ed.: W. J. Orville-Thomas), Wiley, London, **1974**.
[15] S. J. Bell, *Mol. Struct.* **1994**, *320*, 125.
[16] A. L. L. East, L. Radom, *J. Chem. Phys.* **1997**, *106*, 6655.
[17] K. S. Pitzer, W. D. Gwinn, *J. Chem. Phys.* **1942**, *10*, 428.
[18] A $\Delta_p S^\circ$ value of $+5\,J\,mol^{-1}K^{-1}$ was suggested in ref. [5c] for the phenol molecule. This estimate is based on the approximation $S^\circ(\text{phenolH}^+) \approx S^\circ(\text{aniline})$; it is not clear that this equality holds, since the most stable protonated form of the phenol is a *C*-protonated structure, not the *O*-protonated one (for which the analogy with aniline was expected to apply). Therefore the GB and PA values discussed here are slightly at variance from that of ref. [5c].

Received: December 28, 2001 [F3769]